Dewetting of Linear Polymer/Star Polymer Blend Film

Lin Xu,[†,‡] Xifei Yu,[†] Tongfei Shi,*[,†] and Lijia An*[,†]

State Key Laboratory of Polymer Physics and Chemistry, Changchun Institute of Applied Chemistry, Chinese Academy of Sciences, Changchun 130022, P. R. China, and Graduate University of the Chinese Academy of Sciences, Beijing, 100049, P. R. China

Received September 21, 2007
Revised Manuscript Received November 27, 2007

Thin polymer films on solid substrates have been widely applied in industrial processing and manufacturing. The film instability is an important factor in its technological applications. The unstable process is called the dewetting process. Recently, there have been many studies reported on the dewetting process by experiments, simulations, and theories.[1−14] Dewetting is mainly induced by two different mechanisms: (1) spinodal dewetting and (2) nucleation and growth. The rupture of films by nucleation strongly depends on the initial conditions. The air bubbles, other defects, and the occurrence of strain in the films can lead to the formation of holes by heterogeneous nucleation. The breakup of films by spinodal dewetting is limited. Recently, a lot of papers have reported spinodal dewetting in experiments, simulations, and theories.[15−21] Besides, Bischof et al.[22] have observed two coexisting mechanisms of nucleation and surface undulation in the dewetting process of the thin metallic film. Thiele et al.[23] also reported a combination of nucleation growth and spinodal dewetting in the dewetting process of evaporating collagen solutions. Xie et al.[24] showed both holes and surface undulation form over a large part of the surface in the 12.5 nm thick polystyrene (PS) film.

Thin polymer blend films are of special interest for technological applications as well as for fundamental investigations. This has motivated many fundamental studies about the phase separation and dewetting of the polymer blend film.[25−31] The macromolecular architecture can influence the wetting property of the polymer film. Krishnan et al.[32] have shown that the addition of PS nanoparticles to thin linear PS film inhibits and in some cases eliminates dewetting because an enriched layer of PS nanoparticles is present on the substrate surface. The different macromolecular architecture can lead their blend film to divide into two-enriched layers. The bilayer film shows a richer dynamics than a one-layer system.[33−39] The instability phenomenon is driven by the effective molecular interactions acting between all the interfaces which separate the four media: substrate, bottom layer, top layer, and surrounding gas (air). In this communication, avoiding all difficulties related with the sample preparation via flotation, we present a bilayer formation via phase separation. We add a four-arm poly(4-vinylbenzyl chloride) (pVBC) into the linear PS film to study the dewetting process of their blend film on the silanized Si wafer. It is found that the addition of four-arm pVBC leads to the formation of a bilayer structure during the spin-coating process. Although the breakup of film is driven by heterogeneous nucleation in pure linear PS film and pure four-arm pVBC film, both heterogeneous nucleation and surface undulation are found in the dewetting process of their blend film on the silanized Si wafer.

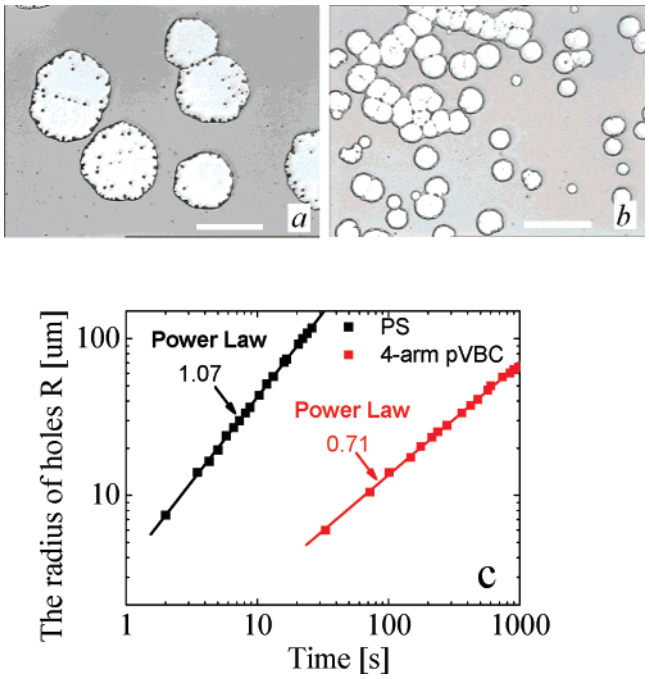

Figure 1. The OM images of (a) the linear PS film treated at 170 °C for 35 s and (b) the four-arm pVBC film treated at 170 °C for 15 min, and the dynamics of their hole growth (c). The bar scale is 100 μm.

The linear PS (M_w = 23 600 g/mol, M_w/M_n = 1.06, the bulk glass transition temperature T_g = 95 °C, supplier TCI) and the four-arm pVBC (M_w = 30 000 g/mol, M_w/M_n = 1.1, the bulk glass transition temperature T_g = 101 °C), which was synthesized by RAFT polymerization, were dissolved in chloroform. Thin polymer films were prepared by spin-coating the chloroform solution onto the Si wafers, which have been silanized (trimethylchlorosilane) prior to use following standard procedures.[40,41] The thickness of film was measured by ellipsometry (JOBIN YVON S.A.S., France). The residual solvent was removed by putting the films in a vacuum oven for 24 h at room temperature, and the surface roughness of the films (below 0.9 nm) was measured by atomic force microscopy (AFM) operating in the tapping mode using a SPA300HV instrument with a SPI3800N controller (Seiko Instruments Inc., Japan). Then, the samples were heated at 120 and 170 °C. The surface morphology was observed by optical microscopy (OM, Leica Microsystems, Germany) in the reflection mode with a CCD camera attachment and atomic force microscopy (AFM) at room temperature. Surface chemical composition of the films was determined on a Thermo ESCALAB 250 X-ray photoelectron spectrometer (XPS) at room temperature and at 10^{-10} Torr. A nonmonochromatized Al Kα excitation source was used. The takeoff angle (between the sample surface and the detector optics) was 90°. We obtained the contact angles of two different liquids on solid surface by drop shape analysis (KRUSS, Germany) at room temperature and used the results to calculate the surface energy of the solid substrate and polymer film by the method of harmonic mean.

* To whom correspondence should be addressed. Email: tfshi@ciac.jl.cn; ljan@ciac.jl.cn. Tel: +86-431-85262137; +86-431-85262206. Fax: +86-431-85262969.
[†] Changchun Institute of Applied Chemistry.
[‡] Graduate University of the Chinese Academy of Sciences.

10.1021/ma702124c CCC: $40.75
Published on Web 12/13/2007

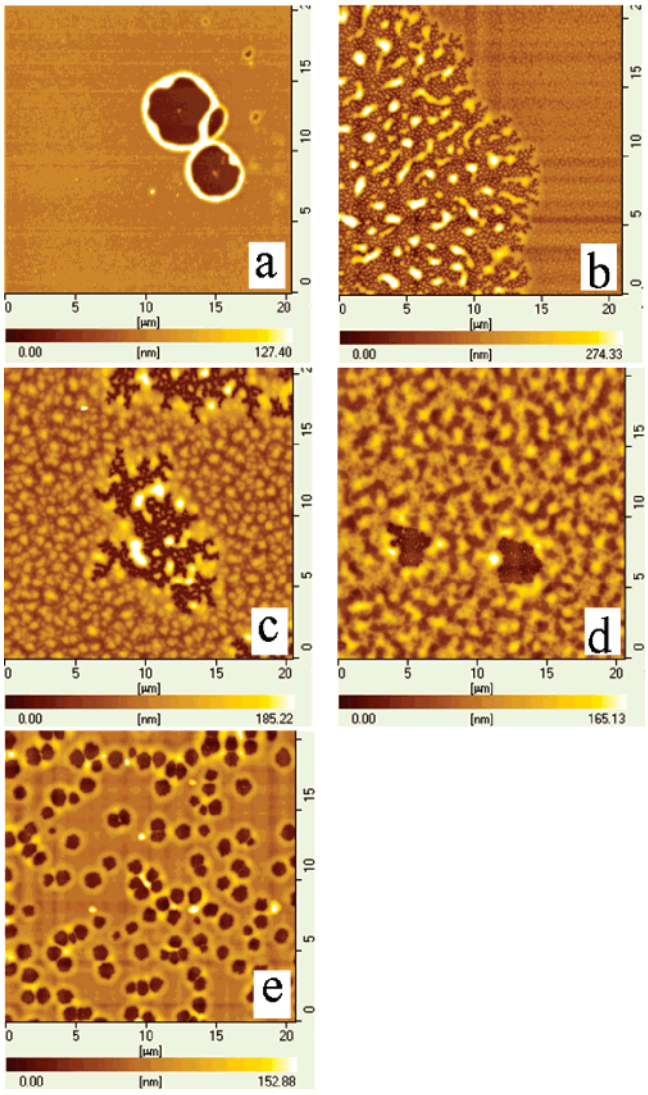

Figure 2. A series of AFM images of the blend films ($h = 28(3)$ nm, in height mode): (a) 10 wt % four-arm pVBC in the blend film at 170 °C for 35 s; (b) 30 wt % four-arm pVBC in the blend film at 170 °C for 2 min; (c) 50 wt % four-arm pVBC in the blend film at 170 °C for 3 min; (d) 70 wt % four-arm pVBC in the blend film at 170 °C for 3 min; (e) 90 wt % four-arm pVBC in the blend film at 170 °C for 3 min.

Figure 1a,b shows the OM images of pure linear PS film and pure four-arm pVBC film ($h = 28(3)$ nm, where h is the film thickness) treated at 170 °C. It can be seen that the rupture of the pure linear PS film and the pure four-arm pVBC film is by heterogeneous nucleation. Figure 1c shows that the radius of the holes grows with time at 170 °C. A theoretical description of the dynamics of hole growth has been reported in previous studies.[4,11,42] The hole radius grows with time as $R \sim t^{2/3}$ if polymer can slip on the substrate, whereas the hole radius grows with time as $R \sim t$ if the slippage condition is not valid. As shown in Figure 1c, the fact that $R \sim t^{1.07}$ for the linear PS film indicates that the slipping effect is not valid and that $R \sim t^{0.71}$ for the four-arm pVBC film implies that the polymer can slip on the substrate. In addition, the dewetting velocity of the linear PS film is faster than that of the four-arm pVBC film on the silanized substrate.

Figure 2 shows a series of AFM images of their blend films ($h = 28(3)$ nm, where h is the film thickness), which are annealed at 170 °C. The morphologies of the blend films with the low (10 wt %) and high (90 wt %) weight contents of the four-arm pVBC are shown in panels a and e of Figure 1. It is observed that the rupture of the films is induced by heterogeneous nucleation. However, both heterogeneous nucleation and surface undulation are found for the polymer blend films with 30, 50, and 70 wt % of the four-arm pVBC (see Figure 1b,c,d).

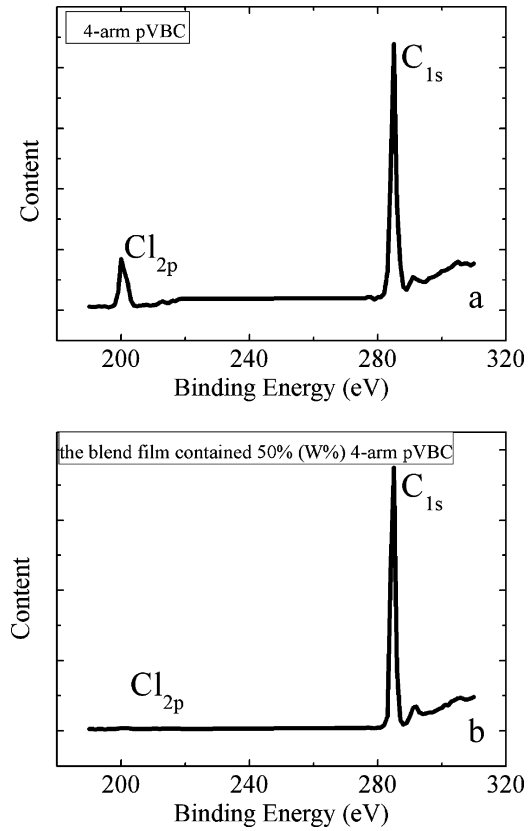

Figure 3. XPS data for: (a) the pure four-arm pVBC film and (b) the blend film containing 50 wt % of four-arm pVBC.

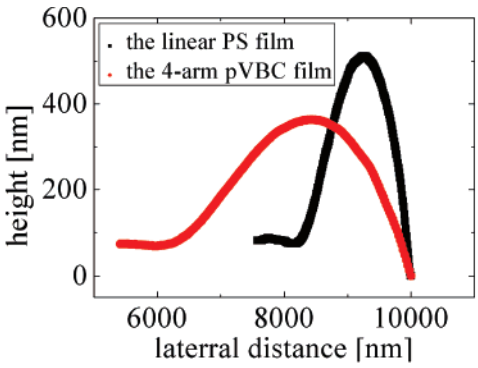

Figure 4. AFM profile images of the rims.

Figure 3 shows the C 1s and Cl 2p region of the XPS spectra. The binding energy peak of C 1s is at 284.6 eV, and the binding energy peak of Cl 2p is at 200 eV. The XPS analysis of the pure four-arm pVBC film before annealing shows that the ratio of the element content of chlorine and the element content of carbon is 1/9.6 on the film surface, but the XPS analysis of the blend film with 50 wt % four-arm pVBC before annealing show that it is 1/13 300 on the film surface (see Figure 3). This indicates that linear PS enriches on the surface of the blend film with 50 wt % four-arm pVBC. The fact implies that the blend film with 50 wt % four-arm pVBC may undergo phase separation and form a bilayer structure during the spin-coating process. In addition, we investigated the receding contact angles of PS on the substrate and four-arm pVBC on the substrate with

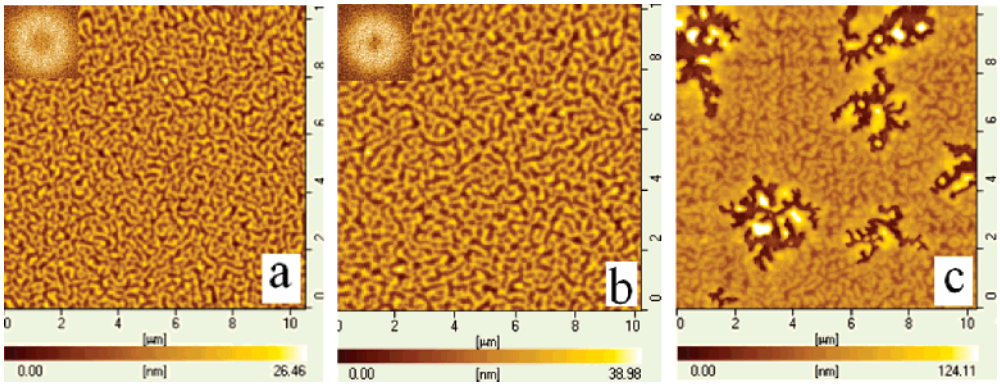

Figure 5. (a) The blend film with 50 wt % of four-arm pVBC annealed at 120 °C for 20 min (2D FFT image shown in the inset). (b) The blend film with 50 wt % of four-arm pVBC annealed at 120 °C for 130 min (2D FFT image shown in the inset). (c) The blend film with 50 wt % of four-arm pVBC annealed at 120 °C for 550 min.

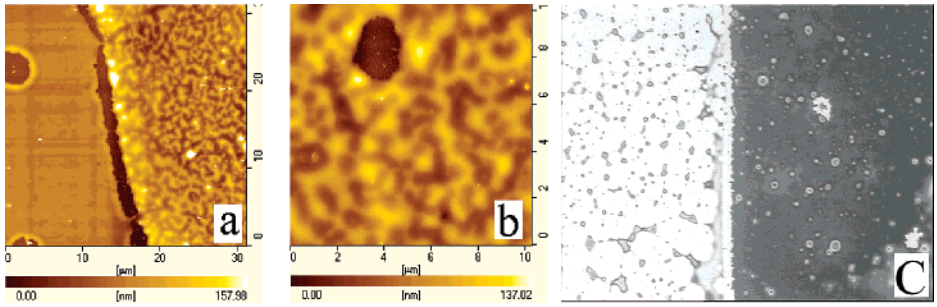

Figure 6. AFM images of (a) The pure four-arm pVBC film (h = 20 nm) treated at 170 °C for 3 min in the left part and the two-layer film, which consists of the linear PS film (h = 15 nm) located on the four-arm pVBC film (h = 20 nm), treated at 170 °C for 3 min in the right part and (b) The two-layer film, which consists of the linear PS film located on the four-arm pVBC film, treated at 170 °C for 3 min. OM image of (c) The pure four-arm pVBC film (h = 20 nm) treated at 170 °C for 60 min in the left part and the two-layer film, which consists of the linear PS film (h = 68 nm) located on the four-arm pVBC film (h = 20 nm), treated at 170 °C for 60 min in the right part. The size of the OM image = 142 μm (height) × 176 μm (width).

the help of the AFM images in order to understand which polymer has more favorable interaction with the substrate. It is obvious that the receding contact angle, θ, of linear PS on the substrate is larger than that of four-arm pVBC on the substrate in the dewetting process (see Figure 4). This indicates that the substrate may have stronger affinity with the four-arm pVBC than with the linear PS. This is consistent with the XPS data. Thus, we predict that a bilayer structure, in which the linear PS enriched layer is located on the four-arm pVBC enriched layer, is formed during the spin-coating process. When the temperature reaches 170 °C, first the spinodal dewetting of the upper linear PS layer occurs on the lower four-arm pVBC layer and then the lower four-arm pVBC layer forms holes on the silanized Si wafer. Due to the slip effect, the moving velocity of the thin region is faster than that of the thick region. Thus, the growth of the holes is irregular. The phenomena in the blend films with 30 and 70 wt % of the four-arm pVBC are similar to that in the blend film with 50 wt %. Therefore, they may have the same dewetting process at 170 °C. The above dewetting process has not been observed for the blend films with 10 and 90 wt % of the four-arm pVBC because the content of the four-arm pVBC or linear PS, respectively, is too low to form a enriched layer.

We explore the dewetting process of the blend film with 50 wt % of the four-arm pVBC at a lower temperature 120 °C because the velocity of dewetting is too fast to observe the process at 170 °C. Figure 5 shows the morphologies of the blend with 50 wt % four-arm pVBC after different annealing times at 120 °C. It is seen that first the film occurs spinodal dewetting and then the holes form and grow irregularly. The dewetting processes at 120 °C give a good evidence for our above explanation.

For the film system under consideration, the total excess free energy ϕ can be expressed as a sum of dispersion energies and polar interactions as follows:[17,23]

$$\phi = -A_{123}/12\pi h^2 + S_p \exp(-h/l) \quad (1)$$

where h is the film thickness, A_{123} is the effective Hamaker constant (1, substrate; 2, medium; 3, film), S_p is the polar component of the spreading coefficient, and l is the correlation length, which is often taken as 2.78 nm. The dispersion energies (the first term in eq 1) can be obtained from the effective Hamaker constant and film thickness. For the three layers being involved, the effective Hamaker constant can be expressed in terms of the dispersion component of each surface tension as:[16]

$$A_{123} = (\sqrt{A_{11}} - \sqrt{A_{33}})(\sqrt{A_{22}} - \sqrt{A_{33}}) = 24\pi d_0^2(\sqrt{\gamma_1^d} - \sqrt{\gamma_3^d})(\sqrt{\gamma_2^d} - \sqrt{\gamma_3^d}) \quad (2)$$

where d_0 is the atomic cutoff length, which is taken as 0.158 nm. The medium phase is pure air (γ_2^d = 0). The polar component of the spreading coefficient was calculated based on the relationship:[23]

$$S = S_d + S_p = \gamma_{23}(\cos\theta - 1) \quad (3)$$

where the dispersion component is given by $-A_{123}/12\pi d_0^2$. γ_{ps} = 28.936 mN/m, γ_{ps}^d = 28.28 mN/m, $\gamma_{\text{four-arm pVBC}}$ = 32.67

mN/m, $\gamma_{\text{four-arm pVBC}}{}^{d} = 31.77$ mN/m, $\gamma_{\text{silanizedSiwafer}} = 20.14$ mN/m, $\gamma_{\text{silanizedSiwafer}}{}^{d} = 17.79$ mN/m, $\theta_{\text{ps/silanizedSiwafer}} = 48°$,[43] $\theta_{\text{four-arm pVBC/silanized Siwafer}} = 42°$,[43] and $\theta_{\text{ps/four-arm pVBC}} = 18°$.[43] From these values, we can yield $S_{\text{ps/silanizedSiwafer}}{}^{d} = -11.7$ mN/m, $S_{\text{ps/silanizedSiwafer}}{}^{p} = 2.126$ mN/m, $S_{\text{four-arm pVBC/silanizedSiwafer}}{}^{d} = -15.98$ mN/m, $S_{\text{four-arm pVBC/silanizedSiwafer}}{}^{p} = 7.589$ mN/m, $S_{\text{ps/four-arm pVBC}}{}^{d} = 3.387$ mN/m, and $S_{\text{ps/four-arm pVBC}}{}^{p} = -4.987$ mN/m. For linear PS film and four-arm pVBC film on the silanized Si wafer, the apolar part of the interaction is an instable term whereas the polar part of the interaction stabilizes the film. For linear PS film on four-arm pVBC film, the apolar part of the interaction is a stable term whereas the polar part of the interaction makes the linear PS film unstable. For the system of linear PS film on four-arm pVBC film, the spinodal parameter $\partial^2\phi/\partial h^2$ is calculated, and $\partial^2\phi/\partial h^2 = -3.1 \times 10^{12}$ J/m^4 < 0 (the thickness of linear PS film is assumed to 15 nm). A negative spinodal parameter leads to spinodal dewetting. These calculated results support the above explanation.

In order to further prove our above explanation, a control experiment was carried out as described below. The linear PS films (film thickness $h = 15$ nm) were floated on the four-arm pVBC films (film thickness $h = 20$ nm). The two-layer films were annealed at 170 °C. The rupture of pure four-arm pVBC film ($h = 20$ nm) is induced by heterogeneous nucleation (as can be seen in the left part of Figure 6a). In the two-layer film, first the upper linear PS layer dewets on the lower four-arm pVBC layer by spinodal dewetting and then the lower four-arm pVBC layer forms holes on the silanized Si wafer (see the right part of the panels a and b of Figure 6). The dewetting process of the two-layer film is similar to that of their blend film at 170 °C. This experiment also supports our above explanation. The linear PS films (film thickness $h = 68$ nm) were floated on the four-arm pVBC films (film thickness $h = 20$ nm). The two-layer films were annealed at 170 °C. The breakup of the two-layer film is by heterogeneous nucleation (as can be seen in Figure 6c).

In summary, the breakup of the film is by nucleation growth in pure linear PS film and pure four-arm pVBC film, but the change of the composition in the blend film leads to different dewetting processes. Dewetting processes in the blend film with low and high content of the four-arm pVBC are through heterogeneous nucleation processes. However, in the blend films with the content of the four-arm pVBC in between the above extremes, they first undergo phase separation and then form a bilayered structure during the spin-coating process. When the temperature reaches above the T_g of polymer, the upper linear PS enriched layer dewets on the lower four-arm pVBC enriched layer by spinodal dewetting and then the lower four-arm pVBC enriched layer forms holes on the silanized Si wafer, which grow irregularly.

Acknowledgment. This work is supported by the National Natural Science Foundation of China (50503022) Programs and the Fund for Creative Research Groups (50621302) and subsidized by the Special Funds for National Basic Research Program of China (2003CB615600).

References and Notes

(1) Sharma, A.; Reiter, G. *J. Colloid Interface Sci.* **1996**, *178*, 383.
(2) Becker, J.; Grün, G.; Seemann, R.; Mantz, H.; Jacobs, K.; Mecke, K.; Blossey, A. *Nat. Mater.* **2003**, *2*, 59.
(3) Gabriele, S.; Sclavons, S.; Reiter, G.; Damman, P. *Phys. Rev. Lett.* **2006**, *96*, 156105.
(4) Jacobs, K.; Seemann, R.; Schatz, G.; Herminghaus, S. *Langmuir* **1998**, *14*, 4961.
(5) Masson, J.-L.; Green, P. F. *Phys. Rev. E* **2002**, *65*, 031806.
(6) Kargupta, K.; Sharma, A. *J. Colloid Interface Sci.* **2002**, *245*, 99.
(7) Müeller-Buschbaum, P. *J. Phys.: Condens. Matter* **2003**, *15*, R1549.
(8) Karapanagiotis, I.; Gerberich, W. W. *Surf. Sci.* **2005**, *594*, 192.
(9) Yang, M. H.; Hou, S. Y.; Chang, Y. L.; Yang, A. C.-M. *Phys. Rev. Lett.* **2006**, *96*, 066105.
(10) Seemann, R.; Herminghaus, S.; Jacobs, K. *J. Phys.: Condens. Matter* **2001**, *13*, 4925.
(11) Brochard-wyart, F.; Debregeas, G.; Fondecave, R.; Martin, P. *Macromolecules* **1997**, *30*, 1211.
(12) Luo, H.; Gersappe, D. *Macromolecules* **2004**, *37*, 5792.
(13) Yoon, B. K.; Huh, J.; Kim, H.-C.; Hong, J.-M.; Park, C. *Macromolecules* **2006**, *39*, 901.
(14) Gabriele, S.; Damman, P.; Sclavons, S.; Desprez, S.; Coppée, S.; Reiter, G.; Hamieh, M.; Akhrass, S. A.; Vilmin, T.; Raphaël, E. *J. Polym. Sci., Part B: Polym. Phys.* **2006**, *44*, 3022.
(15) Reiter, G. *Phys. Rev. Lett.* **1992**, *68*, 75.
(16) Reiter, G.; Sharma, A.; Khanna, R.; Casoli, A.; David, M.-O. *J. Colloid Interface Sci.* **1999**, *214*, 126.
(17) (a) Sharma, A.; Khanna, R. *J. Chem. Phys.* **1999**, *110*, 4929. (b) Sharma, A.; Khanna, R. *Phys. Rev. Lett.* **1998**, *81*, 3463.
(18) Seemann, R.; Herminghaus, S.; Jacobs, K. *Phys. Rev. Lett.* **2001**, *86*, 5534.
(19) Suh, K. Y.; Lee, H. H. *Phys. Rev. Lett.* **2001**, *87*, 135502-1.
(20) Pismen, L. M. *Phys. Rev. E* **2004**, *70*, 021601.
(21) Mitlin, V. *J. Colloid Interface Sci.* **2005**, *281*, 444.
(22) Bischof, J.; Scherer, D.; Herminghaus, S.; Leiderer, P. *Phys. Rev. Lett.* **1996**, *77*, 1536.
(23) Thiele, U.; Mertig, M.; Pompe, W. *Phys. Rev. Lett.* **1998**, *80*, 2869.
(24) Xie, R.; Karim, A.; Douglas, J. F.; Han, C. C.; Weiss, R. A. *Phys. Rev. Lett.* **1998**, *81*, 1251.
(25) Müller-Buschaum, P.; Cubitt, R.; Petry, W. *Appl. Phys. A: Mater. Sci. Process.* **2002**, *74*, S342.
(26) Müller-Buschaum, P.; O'Neill, S. A.; Affrossman, S.; Stamm, M. *Macromolecules* **1998**, *31*, 5003.
(27) Müller-Buschaum, P.; Gutmann, J. S.; Stamm, M. *Macromolecules* **2000**, *33*, 4886.
(28) Müller-Buschaum, P.; Gutmann, J. S.; Stamm, M.; Cubitt, R.; Cunis, S.; von Krosigk, G.; Gehrke, R.; Petry, W. *Physica B* **2000**, *283*, 53.
(29) Chung, H.-j.; Wang, H.; Composto, J. R. *Macromolecules* **2006**, *39*, 153.
(30) Chung, H.-j.; Ohno, K.; Fukuda, T.; Composto, J. R. *Macromolecules* **2007**, *40*, 384.
(31) Liao, Y.; Su, Z.; Sun, Z.; Shi, T.; An, L. *Macromol. Rapid Commun.* **2006**, *27*, 351.
(32) Krishnan, R. S.; Mackay, M. E.; Hawker, C. J.; Horn, B. V. *Langmuir* **2005**, *21*, 5770.
(33) Brochard-wyart, F.; Martin, P.; Redon, C. *Langmuir* **1993**, *9*, 3682.
(34) Karusch, G. *J. Phys.: Condens. Matter* **1997**, *9*, 7741.
(35) Lambooy, P.; Phelan, K. C.; Haugg, O.; Krausch, G. *Phys. Rev. Lett.* **1996**, *76*, 1110.
(36) Renger, C.; Müller-Buschbaum, P.; Stamm, M.; Hinrichsen, G. *Macromolecules* **2000**, *33*, 8388.
(37) (a) Pototsky, A.; Bestehorn, M.; Merkt, D.; Thiele, U. *Phys. Rev. E* **2004**, *70*, 025201(R). (b) Pototsky, A.; Bestehorn, M.; Merkt, D.; Thiele, U. *J. Chem. Phys.* **2005**, *122*, 224711.
(38) Govor, L. V.; Reiter, G.; Bauer, G. H.; Parisi, J. *Appl. Phys. Lett.* **2006**, *89*, 133126.
(39) de Silva, J. P.; Geoghegan, M.; Higgins, A. M.; Krausch, G.; David, M.-O.; Reiter, G. *Phys. Rev. Lett.* **2007**, *98*, 267802.
(40) Wasserman, S. R.; Tao, Y.; Whitesides, G. M. *Langmuir* **1989**, *5*, 1075.
(41) Brzoska, J. B.; Ben Azouz, I.; Rondelez, F. *Langmuir* **1994**, *10*, 4367.
(42) Brochard-wyart, F.; de Gennes, P.-G.; Hervert, H.; Redon, C. *Langmuir* **1994**, *10*, 1566.
(43) Sehgal, A.; Ferreiro, V.; Douglas, J. F.; Amis, E. J.; Karim, A. *Langmuir* **2002**, *18*, 7041.

MA702124C